Biochemical Society Transactions (2019) **47** 1197–1207
https://doi.org/10.1042/BST20190316

Review Article

Glutamate transporters: a broad review of the most recent archaeal and human structures

Ana Pavić[1,2,*], Alexandra O. M. Holmes[1,*], Vincent L. G. Postis[1,2] and Adrian Goldman[1,3]

[1]Astbury Centre for Structural Molecular Biology, School of Biomedical Sciences, University of Leeds, Leeds, U.K.; [2]Biomedical Research group, School of Clinical and Applied Sciences, Leeds Beckett University, Leeds, U.K.; [3]Faculty of Biological and Environmental Sciences, University of Helsinki, Helsinki, Finland

Correspondence: Adrian Goldman (a.goldman@leeds.ac.uk)

Glutamate transporters play important roles in bacteria, archaea and eukaryotes. Their function in the mammalian central nervous system is essential for preventing excitotoxicity, and their dysregulation is implicated in many diseases, such as epilepsy and Alzheimer's. Elucidating their transport mechanism would further the understanding of these transporters and promote drug design as they provide compelling targets for understanding the pathophysiology of diseases and may have a direct role in the treatment of conditions involving glutamate excitotoxicity. This review outlines the insights into the transport cycle, uncoupled chloride conductance and modulation, as well as identifying areas that require further investigation.

Introduction

Glutamate is the most important excitatory transmitter in the brain. It carries messages between cells that are essential for normal development and function related to learning and memory. Additionally, glutamate molecules can promote connections among brain cells and remove unnecessary ones [1].

Glutamate transporters, also called Excitatory Amino Acid Transporters (EAATs), are members of the solute carrier 1 (SLC1) family of the secondary active transporters' important targets for drug development. SLC1 includes a range of human and prokaryotic glutamate and aspartate transporters, and two neutral amino acid transporters Alanine Serine Cysteine Transporters 1 and 2 (ASCT1 and 2) [1]. The five human glutamate transporters (EAAT1-5) are expressed abundantly throughout the central nervous system [2]. Glutamate transporters are responsible for ensuring that glutamate is constantly pumped into the cytoplasm, thus preventing cytotoxicity and neural damage. Eukaryotic glutamate transporters are the secondary active transporters as they couple the influx of one glutamate, three sodium ions and one proton with the efflux of one potassium ion [3] (Figure 1A). In addition, eukaryotic glutamate transporters exhibit thermodynamically uncoupled chloride conductance resulting in an overall uncoupled glutamate-gated anion channel activity [4–6]. Archaeal transporter homologues are highly selective for aspartate over glutamate and, unlike EAATs, transport does not depend on proton or potassium gradients [7] (Figure 1B). ASCTs, a structurally related family, mediate Na^+-dependent exchange of small neutral amino acids at the plasma membrane [3]. Like the EAATs, archaeal homologues and ASCTs exhibit uncoupled anion conductance [8,9].

As the major excitatory transmitter, glutamate has a key role in the pathogenesis of different neurological disorders [1]: excess extracellular glutamate is toxic to the surrounding neurons via overstimulation that can result in cell damage and/or death. This has been linked to epilepsy, episodic ataxia, schizophrenia and Alzheimer's disease [10], and so EAATs have attracted much attention as they represent targets for understanding and treating these disorders [11].

The best structurally characterized members of SLC1 transporters are archaeal homologues Glt_{Ph} and Glt_{Tk} [12–21] (Table 1). They share ~36% sequence identity with eukaryotic EAATs [22] with many conserved residues involved in substrate and ion binding and transport [13]. The progress in crystallographic studies of the glutamate transporter family, including the structure of human EAAT1

*These authors contributed equally to this work.

Received: 12 April 2019
Revised: 11 July 2019
Accepted: 15 July 2019

Version of Record published: 5 August 2019

Biochemical Society Transactions (2019) **47** 1197–1207
https://doi.org/10.1042/BST20190316

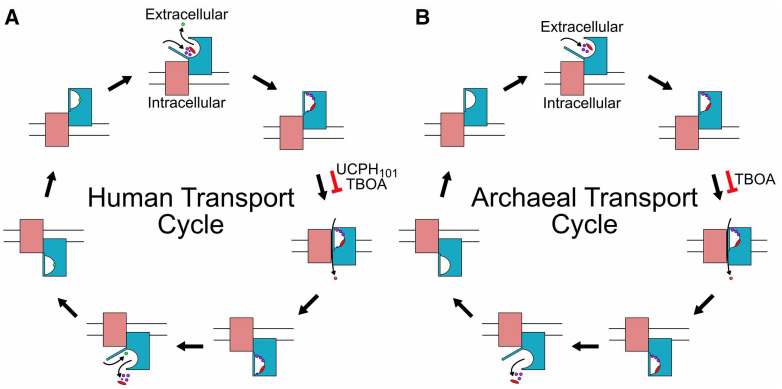

Figure 1. Human and archaeal glutamate or aspartate transport cycles.

(**A**) The transport of one glutamate (red) is coupled to the co-transport of three Na^+ (purple) and one proton (blue), and the counter-transport of one K^+ in the case of the human transport cycle. (**B**) The archaeal transport cycle is similar but involves the coupled transport of one aspartate (red) and 3 Na^+ (purple) with no counter-transport. One of the intermediate transport conformations of the transporter forms an anion permeation pathway to allow uncoupled Cl^- (orange) conductance. Both the negative allosteric modulator UCPH101 and the competitive inhibitor TBOA prevent the transporter from changing from the outward-facing conformation to the inward-facing conformation. For clarity, only single subunit (scaffold domain in pink and transport domain in blue) is shown in the membrane plane.

[23], has revealed much about the mechanism of glutamate transporters. The recent structure of glutamine transporter ASCT2 solved by cryo-EM [24] (Table 1), resembles of Glt_{Ph} and Glt_{Tk} and EAAT1 structures and reveals differences in substrate specificity as well as transport modes between ASCT2 and EAAT1.

This review summarizes the current understanding of the structure, transport and modulation mechanisms of glutamate transporters, highlighting what remains to be discovered and how that might be achieved.

Structure of glutamate transporters

Glutamate transporters are typically homotrimeric [13,25,26] (Figure 2), although EAAT3 and EAAT4 may also co-assemble as a heterotrimer [27]. The existence of a trimeric structure was first hypothesized on the basis of the archaeal glutamate transporter homologue Glt_{Ph} [7,13], and the first crystal structure of the human EAAT1 [23] shown of a symmetric homotrimer in an outward-facing conformation (OFC) (Table 1).

Each subunit (protomer) of the trimer contains eight α-helical transmembrane segments (TM1-8) and two re-entrant loops, known as helical hairpins (HP1 and HP2). They are arranged into a peripheral 'transport domain' and a central trimerization 'scaffold domain' (Figure 2C). The latter is formed by TM1, TM2, TM4 and TM5 [12,17]. Three scaffold domains form a central structure of the trimer and embed it in the membrane.

TM3, TM6, TM7, TM8 and re-entrant helical hairpins HP1 and HP2 form the peripheral transport domain (Figure 2C). It contains motifs involved in substrate and cation binding. HP1 reaches up to the bottom of the extracellular basin, whereas HP2 is situated almost parallel to the membrane plane, with a large fraction exposed to solvent facing the extracellular basin in the OFC [13]. HP2 controls substrate and ion access to their binding sites [23].

The recently solved cryo-EM structure of ASCT2 [24] is highly similar to structures of other SLC1 members, although EAAT1 and ASCT2 scaffold domain have different orientations relative to the scaffold domain [24].

Sodium- and aspartate-binding sites

The structures of *holo* and *apo* Glt_{Tk} allowed the identification of the sodium- and substrate-binding sites (Table 1) [20]. Na1, on the cytoplasmic side below the transported aspartate, is stabilized by the conserved Asp409 side chain on TM8 and main-chain carbonyl groups from the central region of TM7 (Gly309, Asn313) and TM8 (Asn405) (Figure 3C). Na2 is just under the re-entrant hairpin motif HP2 (above the transported aspartate, nearer the extracellular side) and is coordinated by the main chain carbonyls of TM7 (Met314) and of HP2 (Ser352, Ile353, Thr355) (Figure 3D) connecting TM7 and TM8. Na3 (Figure 3E) is between the

Table 1 Selected glutamate transporter structures Part 1 of 2

PDB ID code	Description	Inward or outward facing	Resolution (Å)	Importance
1XHF [13]	Glt_{Ph} with seven His residues introduced into non-conserved sites on predicted loops	Outward-facing	3.5	• Trimer architecture • Protomer structure • Subunit interface • Oligomerization state
2NWL [12]	Glt_{Ph} in complex with L-Asp	Outward-facing	2.96	• Binding sites for aspartate
2NWX [12]	Glt_{Ph} in complex with L-Asp and Na^+	Outward-facing	3.29	• Sites for sodium ions • Role of HP2
2NWW [12]	Glt_{Ph} in complex with TBOA	Outward-facing	3.2	• TBOA inhibitor site
3KBC [17]	Glt_{Ph} K55C/A364C mutant cross-linked with Hg^{2+} in the presence of Na^+	Inward-facing	3.51	• A mechanism of transporter mediating substrate transport
3V8F [14]	Glt_{Ph} V216C/M3854C mutant cross-linked with Hg^{2+} in the presence of Na^+	Inward-facing	3.8	• Structural principle by which transport intermediates may mediate uncoupled permeation of polar solutes
4IZM [18]	Glt_{Ph} L66CC/S300C mutant cross-linked with divalent mercury; in the presence of aspartate and Na^+	Outward-facing	4.5	• Insights into binding thermodynamics • Chemical potential of sodium ions coupled to substrate binding and release
4P6H [19]	Glt_{Ph} K55C/A364C cross-linked with Hg^{2+} in the presence of Tl^+ bound	Inward-facing	4.08	• The coupling mechanism • A new cation-binding site • Potassium binding stabilizing the conformation of the transport domain
4P1A [19]	Glt_{Ph} K55C/A364C cross-linked with Hg^{2+} in the presence of Tl^+ bound in the *apo* conformation	Inward-facing	3.75	
4P19 [19]	Glt_{Ph} K55C/A364C cross-linked with Hg^{2+} in *apo* conformation	Inward-facing	3.25	
4P3J [19]	Glt_{Ph} K55C/A364C cross-linked with Hg^2 in alkali-free condition in *apo* conformation	Inward-facing	3.5	
5CFY [19]	Glt_{Ph} R397A in complex with Na^+ and L-Asp	Outward-facing	3.5	
5DWY [20]	Substrate free Glt_{Tk}	Outward-facing	2.7	• A structural insight into coupled binding of sodium ions and substrate
5E9S [20]	Substrate bound Glt_{Tk}	Outward-facing	2.8	
4X2S [21]	Glt_{Ph} 276S/M395R with aspartate and Na^+	Intermediate inward-facing	4.21	• An inverse relationship between substrate affinity and transport domain motions
5LLM [23]	Thermostabilized EAAT1 in complex with L-Asp and the allosteric inhibitor $UCPH_{101}$	Outward-facing	3.32	• The first crystal structure of a thermostabilized human EAAT1

Continued

Biochemical Society Transactions (2019) **47** 1197–1207
https://doi.org/10.1042/BST20190316

Table 1 Selected glutamate transporter structures Part 2 of 2

PDB ID code	Description	Inward or outward facing	Resolution (Å)	Importance
5MJU [23]	Thermostabilized EAAT1 in complex with competitive inhibitor TBF-TBOA and the allosteric inhibitor $UCPH_{101}$	Outward-facing	3.71	• Architecture features of human transporters • Molecular mechanism of the function and pharmacology
6R7R [16]	Glt_{Tk} in complex with D-aspartate	Outward-facing	2.8	• Explanation on how geometrically different molecules L- and D-aspartate are recognized and transported by the protein in the same way
6GCT [24]	cryo-EM structure of the human neutral amino acid transporter ASCT2	Inward-facing	3.85	• Details on subtype-specific differences among human SLC1 members

central region of helix 7 that contains a conserved NMDGT motif and TM3 [20] and is coordinated by hydroxyl groups of Thr94 and Ser95 from TM3, the carboxamide group of conserved Asn313 and the side-chain carboxyl of Asp315 and the main chain carbonyl of Tyr91. Despite the names, the order of affinities is Na3 > Na1 > Na2, based on structural and thermodynamic studies [28–30]. For instance, the interaction distances appear to be the shortest for Na3 (~2.2–2.4 Å, in comparison with ~2.5–2.7 Å for Na1 and Na2), indicating that it binds with the highest affinity. Free energy calculations performed in the OFC for the Glt_{Ph} support the assignment of Na3 as the tightest-binding cation [30]. Simulations also suggest that Na2 binds last, after substrate, and has the weakest affinity [29].

The residues in the substrate-binding site of eukaryotic glutamate transporters and archaeal transporter homologues are mostly conserved [12,15,16,23] (Figure 3A,B). The aspartate, situated in the centre of the membrane plane in the OFC, is coordinated by the tips of HP1 and HP2, and side chains on TM7 and TM8 [15]. Thr317 (TM7) interacts with the γ-carboxyl group of the aspartate, the side chain of Asn405 (TM8) and the main chain of Ser280 (HP1) interact with the α-carboxyl group, and the amino group of the aspartate forms contact with the side chain of Asp398 (TM8) and the main chain carbonyl groups of Val358 (HP2) and Arg278 (HP1) (Figure 3A).

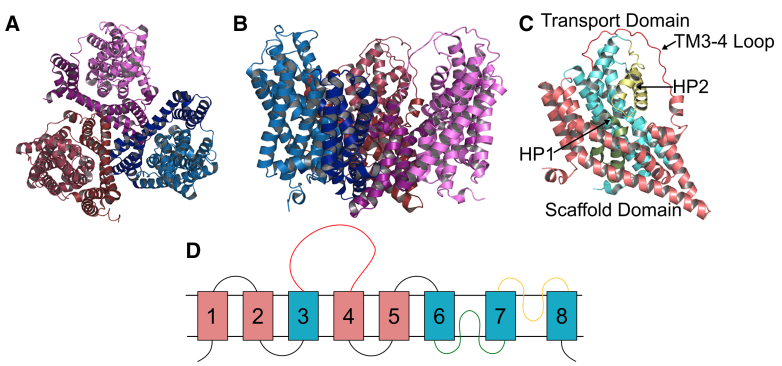

Figure 2. Glutamate transporter structure.
Cartoon representation of the subunits of Glt_{Tk} (PDB: 5E9S) in the outward-facing conformation, where the scaffold domain is shown in a darker shade to the transport domain, viewed from (**A**) the extracellular side and (**B**) the membrane plane. (**C**) The different domains of a single subunit viewed from the trimerization interface and (**D**) topology diagram of one protomer where the scaffold domain is shown in pink (TM1, TM2, TM4, TM5), the transport domain in blue (TM3, TM6, TM7, TM8, HP1, HP2), HP1 is shown in green, HP2 in yellow and the TM3–TM4 loop in red.

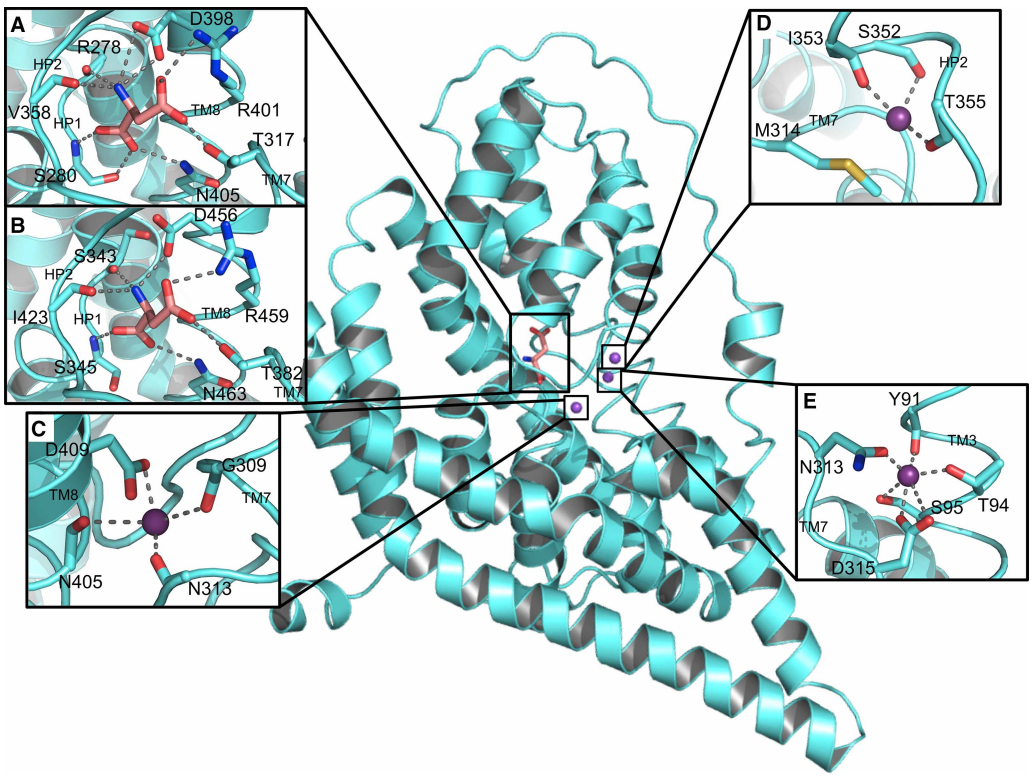

Figure 3. Binding sites in the outward-facing conformation.

The binding of aspartate in (**A**) the Glt_{Tk} (PBD: 5E9S) or (**B**) the human transporter (PDB: 5LM4) structures, (**C–E**) the binding of Na1, Na2, and Na3, respectively, in Glt_{Tk}. The sodium ions are represented as purple spheres and the aspartates or interacting residues as sticks and all are shown in the context of the overall architecture of a single subunit.

Crystal structures of human members of the glutamate transporter family [23,24] showed high similarities among homologues. A crystal structure of an aspartate-bound thermally stabilized mutant of EAAT1 revealed a substrate-binding site nearly identical with that of Glt_{Ph} [23]. The conserved residues on TM8 (Asp456, Arg459 and Asn463) and TM7 (Thr382) coordinate the aspartate identically to the corresponding archaeal amino acids. Despite some differences in amino acids identity on HP1 (Ser343 and Ser345 (human) vs Arg278 and Ser280 (archaea) and HP2 (Ile423 (human) vs Val358 (archaea)), coordination of aspartate via the backbone atoms of these residues is maintained (Figure 3A,B).

Comparison of the glutamine-binding site in ASCT2 and the glutamate-binding site in EAAT1 revealed the structural basis for the differences in the selectivity and binding mechanism of these highly related transporters. The majority of the residues in the binding sites are conserved (Asp464 (456), Asp460 (452), Thr468 (460), Ser353(345), Asn471(463) (EAAT1 numbering in brackets)), but the location of Cys467 in ASCT2 is occupied by Arg459 in EAAT1 and Ala390 is replaced by Thr382 [24]. Site-directed mutagenesis has shown that Cys to Arg substitution alters the selectivity of these transporters from neutral to charged amino acid substrates [31]. Thr382 is essential for the cooperativity of Na^+ and glutamate binding in the concentrative transporter EAAT1, but it has been suggested that this functionality may not be needed in the equilibrative ASCT2 [24].

Cooperative binding mechanism between sodium ions and aspartate

Glutamate transporters have a coupled binding mechanism: the chemical potential of sodium ions is coupled to the binding and release of the substrate. A recent kinetic study described cooperative binding as a key mechanism contributing to coupled transport by Glt_{Ph} [32]. Consistent with a cooperative binding, substrate binding is fast and of high affinity [33] (K_d of 2 nM) in the OFC when the extracellular concentration of Na^+ is high (200 mM) [12].

Biochemical Society Transactions (2019) **47** 1197–1207
https://doi.org/10.1042/BST20190316

In the absence of substrate, HP2 adopts an open conformation, making the substrate-binding site accessible to the extracellular solution [12]. The tip of HP2 is open in the crystal structure of sodium-bound OFC Glt_{Ph} [19], thus preventing uptake of uncoupled sodium ions [12].

Local rearrangements explain the coupling mechanism as shown by binding studies [18,34] and molecular dynamics simulations [29]. The slow and weak binding of two sodium ions [33,34] is associated with transporter core remodelling into a state that enables it to bind substrate and the remaining sodium ion, as shown by a cross-linking approach that trapped the transporter in key conformational states [18]. Aspartate does not bind with measurable affinity in the absence of Na^+ [18]. Kinetic studies confirmed that sodium ion binding occurs before substrate binding, but both one-sodium and two-sodium mechanisms appeared possible [32].

The most striking difference between the *apo* (ligand-free) and *holo* (ligand-bound) OFC structures is the conformation of the conserved NMDGT motif in TM7 [20]. Sodium binding to Asn313 in the Na3 site changes the geometry of the Na1 site to allow another sodium ion to bind, stabilizing the region. Gly316 and Thr317 in the NMDGT motif move closer to TM8 [20]. This, and the Na3 binding-mediated movement of TM3 towards TM7, places Thr317 in the optimal position to bind aspartate and reorients the side chain of Arg401, creating space for the aspartate to bind and allowing the guanidium group to interact with the β-carboxylate of aspartate. The interlinked Na3 and Na1 binding thus increases the affinity for aspartate. Na2 is likely the last site to fill [12], and its binding is coupled to the positioning of Met314 at the centre of the triangle formed by the bound substrate and two sodium ions. These structural changes provide compensatory interactions, allowing the HP2 tip to close [20].

There is no EAAT structure with glutamate bound. Kinetic studies on eukaryotic glutamate transporters show weak binding of 1 or 2 Na^+ ions prior to the binding of the substrate which is followed by the binding of the last Na^+ [35]. Although glutamate and aspartate binding should be similar, molecular dynamics (MD) simulations of homology-modelled EAAT3 suggest that glutamate is not stable in the amino-acid-binding site unless Glu374 is protonated [36]. The co-transported proton appears to be required for glutamate binding and transport. This needs further experimental investigation.

Transport motions

The transport cycle, driven by ionic gradients, involves alternate binding and release of the substrate on the extra- and intracellular sides of the plasma membrane due to the conformational transitions between OFC and IFC [18]. The alternate opening of the extracellular and intracellular gates is strictly maintained: in the OFC, when HP2 opens to expose the substrate and ion-binding sites to the extracellular solution, HP1 is secured in the closed state, packed against TM2 and TM5. Conversely, in the IFC, HP2, the extracellular gate, is locked closed upon displacing HP1 [17] (Figure 1).

Large rigid-body transport domain movements, relative to the static scaffold domain have been observed in the archaeal homologue of glutamate transporters for the first time [21]. The crystal structures of Glt_{Ph} in OFC and IFC [12,13,17,19] showed that, during the transport cycle, the transport domains' elevator-like movements are supported by relatively rigid scaffold domains [17,21]. In the transition between OFC and IFC, the transport domain undergoes large transmembrane movements [37], involving a rotation of 37° and a translation of 15–18 Å that results in the substrate and ion-binding sites facing the cytoplasm [17], with rotation preceding translation. A complex motion between TM2 and TM4 as well as the conformational shift of TM4 may occur [38]. The scaffold domain, however, does not undergo conformational changes: its role is to mediate the intersubunit contacts in the transporter [18].

A single-molecule fluorescence resonance energy transfer study reported that the three Glt_{Ph} subunits undergo independent conformational changes in an unsynchronized manner during aspartate transport [39] in accordance with the biochemical experiments conducted on eukaryotic transporters [40,41]. Furthermore, high-speed atomic force microscopy demonstrated that the protomers in the trimer act independently of each other: there was no correlation between the motions of individual transport domains [42]. Even though there were frequent transitions between OFC and IFC in the *apo* transporter, only one domain was in the IFC at one time [42]. When Na^+ was bound, there was a significant decrease in the fraction of moving protomers: protomers that bound only Na^+ were mostly unable to translocate. On the other hand, Glt_{Ph} translocation dynamics increased when both Na^+ and aspartate were bound [42].

Molecular-level understanding requires comparison of the *apo* and *holo* OFC and IFC structures [21]. In the *apo* form, the transport domain has the same structure in both OFC and IFC [19]. However, the quality of the IFC structures is too poor for steered MD simulations and higher-resolution crystal structures of the

intermediate forms are unlikely, due to the high heterogeneity of conformations and their short life-times. Recent developments in time-resolved electron microscopy [43] may help in this regard.

Substrate release

Once three Na^+ ions and aspartate are bound to the transporter, Na2 is in rapid equilibrium with a solution and its release is required for the disassembly of the complex [32]. Although the mechanism of substrate release is still somewhat unclear, Dechancie and colleagues [44] considered HP1 as the possible IFC-gate controlling element. They suggested that, following transition to the IFC, dissociation of Na2 triggers HP2 loop opening, therefore exposing and hydrating the aspartate and the other sodium ions and destabilizing the interactions between the substrate and the residues on HP2 and TM8. This causes opening of the HP1 loop, disrupting the hydrogen bonds between the Ser277and Ser279 (SSS) motif on HP1 and the substrate and allowing substrate release. As HP2 moves at least 4 Å away from the core, it may serve as the intracellular gate in the IFC [45]. Increase in the distance between TM8 and HP2 enables the substrate rearrangement across the space between HP1, HP2 and TM8. Furthermore, the interaction between the guanidium group of Arg276 at the HP1 and the β-carboxylate of the aspartate promotes the substrate translocation toward the cell interior. More recent Glt_{Tk} structures with substrate and sodium ions bound showed that the loop between TM3 and TM4 (Figure 2C), important in the transport, appeared to restrict HP2 movement in the OFC [20]. This may also occur in the IFC.

In ASCT2, the tip of HP2 is located on the cytoplasmic side of the membrane and, as it is not packed against the scaffold domain, HP2 in the IFC might possibly open in a similar manner as has been shown for Glt_{Ph} and EAAT1 in the OFC [24]. Therefore, a single gate might alternately allow access from both sides of the membrane, without the need for HP1 opening [24].

Molecular dynamics and free energy calculations on the inward-facing conformation (IFC) of Glt_{Ph} predicted that unbinding occurs as follows: Na2 → gate opening → Asp → Na1 → Na3 [28], with Na3 release being rate limiting. After ligand release, the *apo* transport domain adopts a compact, occluded conformation that can traverse the membrane, completing the transport cycle. Interactions between HP1, HP2, TM7 and TM8 stabilize the *apo* conformation [19]. Higher-resolution structures of the IFC will be required to determine the identity of the intracellular gate and mechanism of substrate release in more detail.

Potassium counter-transport

Human EAATs must counter-transport a K^+ to the extracellular medium for the reorientation from the IFC to the OFC [3]. Potassium binding to the IFC has been proposed to enable translocation of the substrate-free transport domain to the OFC [19]. Verdon and colleagues claimed to identify a potassium-binding site in Glt_{Ph} [19], but subsequent structure analysis led to this being disregarded [22].

MD simulations on homology-modelled EAAT3 [36] suggested that a site close to the Na1 and Na3-binding sites (Figure 3) was the most likely as it had the highest affinity of the three considered. However, the K^+ ion was placed directly in the putative site, so the accessibility of binding sites and potential conformational changes between *apo* and *holo* forms was ignored. This is relevant because one of the sites was near several positively charged residues, which could prevent K^+ entering and binding. The simulations were also just 50 ns, so the ion position was not stable.

Confirmation of any of these binding sites requires a structure of the *holo* complex, which is not yet available [23]. Moreover, the domain motions following K^+ binding leading to the relocation to the OFC need to be defined.

Uncoupled chloride conductance

The chloride conduction pathway and the mechanism of anion permeation are still not completely understood. The anion selectivity of Glt_{Ph}, the main subject of anion conductance studies, is almost identical with that of EAATs [46]. Chloride permeation occurs at the interface between the scaffold and transport domains, but it is not clear what conformational state mediates anion permeation nor exactly which residues are involved.

Initially, chloride permeation was proposed to occur along TM2 [47]. The Ser to Val mutation on TM2 (residue 65 in Glt_{Ph} and 103 in EAAT1) strongly affected chloride permeation [8,47]. The Glt_{Ph} structure in an intermediate OFC suggested that there was an aqueous cavity that might serve as a permeation pathway for anions [14]. Subsequent research has suggested that substrate transport and anion permeation proceed through two mutually exclusive pathways separated by a flexible wall domain [48] and facilitated by the conformational

Biochemical Society Transactions (2019) **47** 1197–1207
https://doi.org/10.1042/BST20190316

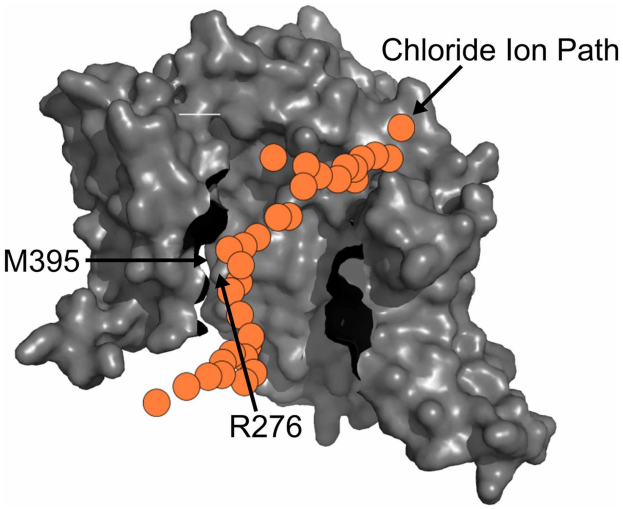

Figure 4. Predicted anion permeation pathway.

A Glt_{Ph} monomer viewed from the trimerization interface. The residues R276 and M395 responsible for the anion selectivity are indicated. The orange circles represent 'snapshots' of the path of a chloride ion through the channel between the two domains. Part of the scaffold domain has been removed for clarity.

changes [49]. The moving flexible wall is composed of several residues in HP1, HP2 hairpins and TM8 (Figure 4), the movement of which dictate the pathway [48]. Arg276 in HP1 and Met395, predicted to line the anion pore [50], were shown to exhibit a significant Cl^- selectivity over Na^+ in both simulations and experiments: anion selectivity is impaired by the insertion of negatively charged side chains at specific positions. In contrast with previous research [48], mutations of Ser65 did not affect anion permeation. Presumably, therefore, Ser65 (Ser103) is part of the channel-opening mechanism but not of the permeation pathway. As the permeation pathway accounted for all known functional properties of EAAT/Glt_{Ph} anion channels during simulations, it is the most likely mechanism of uncoupled chloride conductance.

Overall, it appears that both archaeal and mammalian transporters generate an open channel and permeation pathway through the cooperative dislocation of a flexible wall during the lateral movement of the transport core. The structural data obtained for anion conductance may be important for designing glutamate transporter anion channel modulators.

Modulation

Modulators are valuable tools for the study of the mechanism of glutamate transport [23]. Initially, the only known modulators were competitive substrate analogues like DL-threo-β-(benzyloxy)aspartic acid (TBOA) [12,23]. The extracellular gate was identified by a crystal structure of Glt_{Ph} in complex with TBOA [12].

The structures of Glt_{Ph} with aspartate and with TBOA are similar (Table 1), as is the conformation of the bound ligands (Figure 5A) [12]. In the TBOA:Glt_{Ph} crystal structure, HP2 is an OFC open conformation, moving from its position in the aspartate-bound complex towards the loop between TM3 and TM4 (Figure 2C). This HP2 movement in the TBOA-bound complex exposes the substrate-binding site to the extracellular solution, suggesting that, in the *apo* state, HP2 adopts an open conformation before aspartate binding [22]. The structure of substrate-free transporter for the Glt_{Tk} homologue revealed an OFC with occluded binding site and closed HP2 [15]. TBOA blocks HP2 in an open conformation, preventing sodium ion binding and subsequent conformational changes and thus inhibiting transport [12].

Selective, allosteric modulators of glutamate transporters are needed: such modulators have great potential to offer insights into the transport mechanism. The best-studied modulator is the non-competitive EAAT1-selective inhibitor $UCPH_{101}$. The structure of thermostabilized EAAT1 in complex with L-aspartate and $UCPH_{101}$ showed that it bound at the scaffold domain-transport domain interface (Figure 5B) [23], over 15 Å from the substrate and sodium-binding sites. $UCPH_{101}$, therefore, does not preclude the movements of HP2 involved in binding of substrate and sodium ions from the extracellular solution. It does, however, induce local and global conformational changes to optimize its coordination in an OFC, thereby preventing transport [23].

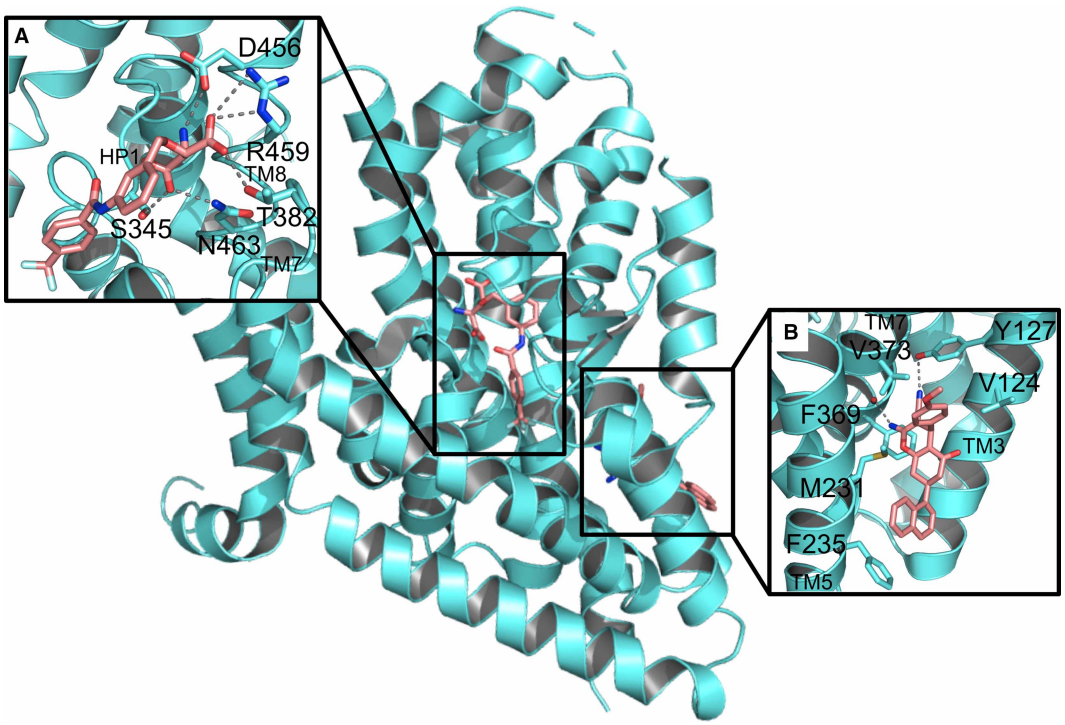

Figure 5. Modulator binding sites of EAAT1.

(**A**) The $TBOA_{TFB}$ (pink) binding site overlaps with the aspartate-binding site as can be seen from its position in the context of a whole subunit. The exact placement of this molecule in structures remains controversial. (**B**) $UCPH_{101}$ binds into a hydrophobic pocket between TM3, 4, and 7 at the interface between the Scaffold and Transport Domains. (PDB: 5MJU).

The structure of $UCPH_{101}$ has provided important insights into the conformational changes in EAAT1 that occur upon binding of substrate and sodium ions. Furthermore, it highlights the importance of allosteric cavities that can facilitate the design of novel, selective compounds — a feature common in membrane proteins [50] (Tate, *pers. comm.*).

Perspectives and future directions

- Mutagenesis, crystallographic and molecular dynamics studies have led to considerable progress in understanding glutamate transporters and their transport dynamics. Recent high-resolution crystal structures of Glt_{Tk} and EAAT1 and cryo-EM structure of ASCT2 have provided new insights into the transport mechanism.

- There are many areas that still require further investigation: glutamate, proton and K^+ binding are still not fully understood and the domain motions triggered by their binding need to be better defined. Our understanding of substrate release, and of the mechanism of potassium counter-transport, remains incomplete. The permeation pathway for chloride ions as well as its relation to substrate transport requires further validation.

- Improved IFC structures, either by X-ray crystallography or by (time-resolved) cryo-electron microscopy should lead to a better understanding. New modulators will further our knowledge of these transporters. We believe that future work will lead to molecules that allow the manipulation of transporter functions and, eventually, the treatment of pathological conditions.

Biochemical Society Transactions (2019) **47** 1197–1207
https://doi.org/10.1042/BST20190316

Abbreviations

ASCT, Alanine Serine Cysteine Transporter; EAATs, Excitatory Amino Acid Transporters; EM, electron microscopy; Glt_{Ph}, *Pyrococcus horikoshii* aspartate transporter; Glt_{Tk}, *Thermococcus kodakarensis* aspartate transporter; HP, helical hairpin; IFC, inward-facing conformation; MD, molecular dynamics; OFC, outward-facing conformation; PBD, protein data bank; SLC, Solute carrier; TBOA, DL-threo-β-(benzyloxy)aspartic acid; TM, transmembrane; $UCPH_{101}$, 2-amino-4-(4-methoxyphenyl)-7-(naphthalen-1-yl)-5-oxo-5,6,7,8-tetrahydro-4H-chromene-3-carbonitrile.

Funding

This work was supported by the Leeds Beckett University fellowship (to V.L.G.P. and A.P.), a BBSRC DTP fellowship (BB/M011151/1) (to A.O.M.H.) the BBSRC (BB/M023281/1), the Academy of Finland (1286429) and by a Royal Society Wolfson fellowship (all to A.G.).

Competing Interests

The Authors declare that there are no competing interests associated with the manuscript.

References

1 Vandenberg, R.J. and Ryan, R.M. (2013) Mechanisms of glutamate transport. *Physiol. Rev.* **93**, 1621–1657 https://doi.org/10.1152/physrev.00007.2013
2 Jensen, A.A., Fahlke, C., Bjørn-Yoshimoto, W.E. and Bunch, L. (2015) Excitatory amino acid transporters: recent insights into molecular mechanisms, novel modes of modulation and new therapeutic possibilities. *Curr. Opin. Pharmacol.* **20**, 116–123 https://doi.org/10.1016/j.coph.2014.10.008
3 Zerangue, N. and Kavanaugh, M.P. (1996) Flux coupling in a neuronal glutamate transporter. *Nature* **383**, 634–637 https://doi.org/10.1038/383634a0
4 Arriza, J.L., Eliasof, S., Kavanaugh, M.P. and Amara, S.G. (1997) Excitatory amino acid transporter 5, a retinal glutamate transporter coupled to a chloride conductance. *Proc. Natl Acad. Sci. U.S.A.* **94**, 4155–4160 https://doi.org/10.1073/pnas.94.8.4155
5 Vandenberg, R.J., Arriza, J.L., Amara, S.G. and Kavanaugh, M.P. (1995) Constitutive ion fluxes and substrate binding domains of human glutamate transporters. *J. Biol. Chem.* **270**, 17668–17671 https://doi.org/10.1074/jbc.270.30.17668
6 Fairman, W.A., Vandenberg, R.J., Arriza, J.L., Kavanaugh, M.P. and Amara, S.G. (1995) An excitatory amino-acid transporter with properties of a ligand-gated chloride channel. *Nature* **375**, 599–603 https://doi.org/10.1038/375599a0
7 Ryan, R.M., Compton, E.L.R. and Mindell, J.A. (2009) Functional characterization of a Na^+-dependent aspartate transporter from *Pyrococcus horikoshii*. *J. Biol. Chem.* **284**, 17540–17548 https://doi.org/10.1074/jbc.M109.005926
8 Ryan, R.M. and Mindell, J.A. (2007) The uncoupled chloride conductance of a bacterial glutamate transporter homolog. *Nat. Struct. Mol. Biol.* **14**, 365–371 https://doi.org/10.1038/nsmb1230
9 Zerangue, N. and Kavanaugh, M.P. (1996) ASCT-1 is a neutral amino acid exchanger with chloride channel activity. *J. Biol. Chem.* **271**, 27991–27994 https://doi.org/10.1074/jbc.271.45.27991
10 Kortagere, S., Mortensen, O.V., Xia, J., Lester, W., Fang, Y., Srikanth, Y. et al. (2018) Identification of novel allosteric modulators of glutamate transporter EAAT2. *ACS Chem. Neurosci.* **9**, 522–534 https://doi.org/10.1021/acschemneuro.7b00308
11 Bröer, S. (2018) Amino acid transporters as disease modifiers and drug targets. *SLAS Discov.* **23**, 303–320 https://doi.org/10.1177/2472555218755629
12 Boudker, O., Ryan, R.M., Yernool, D., Shimamoto, K. and Gouaux, E. (2007) Coupling substrate and ion binding to extracellular gate of a sodium-dependent aspartate transporter. *Nature* **445**, 387–393 https://doi.org/10.1038/nature05455
13 Yernool, D., Boudker, O., Jin, Y. and Gouaux, E. (2004) Structure of a glutamate transporter homologue from *Pyrococcus horikoshii*. *Nature* **431**, 811–818 https://doi.org/10.1038/nature03018
14 Verdon, G. and Boudker, O. (2012) Crystal structure of an asymmetric trimer of a bacterial glutamate transporter homolog. *Nat. Struct. Mol. Biol.* **19**, 355–357 https://doi.org/10.1038/nsmb.2233
15 Jensen, S., Guskov, A., Rempel, S., Hänelt, I. and Slotboom, D.J. (2013) Crystal structure of a substrate-free aspartate transporter. *Nat. Struct. Mol. Biol.* **20**, 1224–1226 https://doi.org/10.1038/nsmb.2663
16 Arkhipova, V., Trinco, G., Ettema, T.W., Jensen, S., Slotboom, D.J. and Guskov, A. (2019) Binding and transport of D-aspartate by the glutamate transporter homolog GltTk. *eLife* **8**, e45286 https://doi.org/10.7554/eLife.45286
17 Reyes, N., Ginter, C. and Boudker, O. (2009) Transport mechanism of a bacterial homologue of glutamate transporters. *Nature* **462**, 880–885 https://doi.org/10.1038/nature08616
18 Reyes, N., Oh, S. and Boudker, O. (2013) Binding thermodynamics of a glutamate transporter homolog. *Nat. Struct. Mol. Biol.* **20**, 634–640 https://doi.org/10.1038/nsmb.2548
19 Verdon, G., Oh, S., Serio, R.N. and Boudker, O. (2014) Coupled ion binding and structural transitions along the transport cycle of glutamate transporters. *eLife* **3**, e02283 https://doi.org/10.7554/eLife.02283
20 Guskov, A., Jensen, S., Faustino, I., Marrink, S.J. and Slotboom, D.J. (2016) Coupled binding mechanism of three sodium ions and aspartate in the glutamate transporter homologue GltTk. *Nat. Commun.* **7**, 13420 https://doi.org/10.1038/ncomms13420
21 Akyuz, N., Georgieva, E.R., Zhou, Z., Stolzenberg, S., Cuendet, M.A., Khelashvili, G. et al. (2015) Transport domain unlocking sets the uptake rate of an aspartate transporter. *Nature* **518**, 68–73 https://doi.org/10.1038/nature14158
22 Arkhipova, V., Guskov, A. and Slotboom, D.-J. (2017) Analysis of the quality of crystallographic data and the limitations of structural models. *J. Gen. Physiol.* **149**, 1091–1103 https://doi.org/10.1085/jgp.201711852

23 Canul-Tec, J.C., Assal, R., Cirri, E., Legrand, P., Brier, S., Chamot-Rooke, J. et al. (2017) Structure and allosteric inhibition of excitatory amino acid transporter 1. *Nature* **544**, 446–451 https://doi.org/10.1038/nature22064
24 Garaeva, A.A., Oostergetel, G.T., Gati, C., Guskov, A., Paulino, C. and Slotboom, D.J. (2018) Cryo-EM structure of the human neutral amino acid transporter ASCT2. *Nat. Struct. Mol. Biol.* **25**, 515–521 https://doi.org/10.1038/s41594-018-0076-y
25 Yernool, D., Boudker, O., Folta-Stogniew, E. and Gouaux, E. (2003) Trimeric subunit stoichiometry of the glutamate transporters from *Bacillus caldotenax* and *Bacillus stearothermophilus*. *Biochemistry* **42**, 12981–12988 https://doi.org/10.1021/bi030161q
26 Gendreau, S., Voswinkel, S., Torres-Salazar, D., Lang, N., Heidtmann, H., Detro-Dassen, S. et al. (2004) A trimeric quaternary structure is conserved in bacterial and human glutamate transporters. *J. Biol. Chem.* **279**, 39505–39512 https://doi.org/10.1074/jbc.M408038200
27 Nothmann, D., Leinenweber, A., Torres-Salazar, D., Kovermann, P., Hotzy, J., Gameiro, A. et al. (2011) Hetero-oligomerization of neuronal glutamate transporters. *J. Biol. Chem.* **286**, 3935–3943 https://doi.org/10.1074/jbc.M110.187492
28 Heinzelmann, G., Bastug, T. and Kuyucak, S. (2013) Mechanism and energetics of ligand release in the aspartate transporter GltPh. *J. Phys. Chem. B* **117**, 5486–5496 https://doi.org/10.1021/jp4010423
29 Bastug, T., Heinzelmann, G., Kuyucak, S., Salim, M., Vandenberg, R.J. and Ryan, R.M. (2012) Position of the third Na^+ site in the aspartate transporter GltPh and the human glutamate transporter, EAAT1. *PLoS ONE* **7**, e33058 https://doi.org/10.1371/journal.pone.0033058
30 Heinzelmann, G., Baştuğ, T. and Kuyucak, S. (2011) Free energy simulations of ligand binding to the aspartate transporter Glt(Ph). *Biophys. J.* **101**, 2380–2388 https://doi.org/10.1016/j.bpj.2011.10.010
31 Bendahan, A., Armon, A., Madani, N., Kavanaugh, M.P. and Kanner, B.I. (2000) Arginine 447 plays a pivotal role in substrate interactions in a neuronal glutamate transporter. *J. Biol. Chem.* **275**, 37436–37442 https://doi.org/10.1074/jbc.M006536200
32 Oh, S. and Boudker, O. (2018) Kinetic mechanism of coupled binding in sodium-aspartate symporter gltPh. *eLife* **7**, e37291 https://doi.org/10.7554/eLife.37291
33 Hänelt, I., Jensen, S., Wunnicke, D. and Slotboom, D.J. (2015) Low affinity and slow Na^+ binding precedes high affinity aspartate binding in the secondary-active transporter GltPh. *J. Biol. Chem.* **290**, 15962–15972 https://doi.org/10.1074/jbc.M115.656876
34 Ewers, D., Becher, T., Machtens, J.-P., Weyand, I. and Fahlke, C. (2013) Induced fit substrate binding to an archeal glutamate transporter homologue. *Proc. Natl Acad. Sci. U.S.A.* **110**, 12486–12491 https://doi.org/10.1073/pnas.1300772110
35 Watzke, N., Bamberg, E. and Grewer, C. (2001) Early intermediates in the transport cycle of the neuronal excitatory amino acid carrier EAAC1. *J. Gen. Physiol.* **117**, 547–562 https://doi.org/10.1085/jgp.117.6.547
36 Heinzelmann, G. and Kuyucak, S. (2014) Molecular dynamics simulations of the mammalian glutamate transporter EAAT3. *PLoS ONE* **9**, e92089 https://doi.org/10.1371/journal.pone.0092089
37 Akyuz, N., Altman, R.B., Blanchard, S.C. and Boudker, O. (2013) Transport dynamics in a glutamate transporter homologue. *Nature* **502**, 114–118 https://doi.org/10.1038/nature12265
38 Rong, X., Tan, F., Wu, X., Zhang, X., Lu, L., Zou, X. et al. (2016) TM4 of the glutamate transporter GLT-1 experiences substrate-induced motion during the transport cycle. *Sci. Rep.* **6**, 34522 https://doi.org/10.1038/srep34522
39 Erkens, G.B., Hänelt, I., Goudsmits, J.M.H., Slotboom, D.J. and van Oijen, A.M. (2013) Unsynchronised subunit motion in single trimeric sodium-coupled aspartate transporters. *Nature* **502**, 119–123 https://doi.org/10.1038/nature12538
40 Grewer, C., Balani, P., Weidenfeller, C., Bartusel, T., Tao, Z. and Rauen, T. (2005) Individual subunits of the glutamate transporter EAAC1 homotrimer function independently of each other. *Biochemistry* **44**, 11913–11923 https://doi.org/10.1021/bi050987n
41 Koch, H.P. and Larsson, H.P. (2005) Small-scale molecular motions accomplish glutamate uptake in human glutamate transporters. *J. Neurosci.* **25**, 1730–1736 https://doi.org/10.1523/JNEUROSCI.4138-04.2005
42 Ruan, Y., Miyagi, A., Wang, X., Chami, M., Boudker, O. and Scheuring, S. (2017) Direct visualization of glutamate transporter elevator mechanism by high-speed AFM. *Proc. Natl Acad. Sci. U.S.A.* **114**, 1584–1588 https://doi.org/10.1073/pnas.1616413114
43 Frank, J. (2017) Time-resolved cryo-electron microscopy: Recent progress. *J. Struct. Biol.* **200**, 303–306 https://doi.org/10.1016/j.jsb.2017.06.005
44 DeChancie, J., Shrivastava, I.H. and Bahar, I. (2011) The mechanism of substrate release by the aspartate transporter GltPh: insights from simulations. *Mol. Biosyst.* **7**, 832–842 https://doi.org/10.1039/C0MB00175A
45 Zomot, E. and Bahar, I. (2013) Intracellular gating in an inward-facing state of aspartate transporter GltPh is regulated by the movements of the helical hairpin HP2. *J. Biol. Chem.* **288**, 8231–8237 https://doi.org/10.1074/jbc.M112.438432
46 Ji, Y., Postis, V.L.G., Wang, Y., Bartlam, M. and Goldman, A. (2016) Transport mechanism of a glutamate transporter homologue GltPh. *Biochem. Soc. Trans.* **44**, 898–904 https://doi.org/10.1042/BST20160055
47 Ryan, R.M., Mitrovic, A.D. and Vandenberg, R.J. (2004) The chloride permeation pathway of a glutamate transporter and its proximity to the glutamate translocation pathway. *J. Biol. Chem.* **279**, 20742–20751 https://doi.org/10.1074/jbc.M304433200
48 Cheng, M.H., Torres-Salazar, D., Gonzalez-Suarez, A.D., Amara, S.G. and Bahar, I. (2017) Substrate transport and anion permeation proceed through distinct pathways in glutamate transporters. *eLife* **6**, e25850 https://doi.org/10.7554/eLife.25850
49 Machtens, J.-P., Kortzak, D., Lansche, C., Leinenweber, A., Kilian, P., Begemann, B. et al. (2015) Mechanisms of anion conduction by coupled glutamate transporters. *Cell* **160**, 542–553 https://doi.org/10.1016/j.cell.2014.12.035
50 Vidilaseris, K., Kiriazis, A., Turku, A., Khattab, A., Johansson, N.G., Leino, T.O. et al. (2019) Asymmetry in catalysis by *Thermotoga maritima* membrane-bound pyrophosphatase demonstrated by a nonphosphorus allosteric inhibitor. *Sci. Adv.* **5**, eaav7574 https://doi.org/10.1126/sciadv.aav7574